



This is a repository copy of *Global analysis of urinary extracellular vesicle small RNAs in autosomal dominant polycystic kidney disease*.

White Rose Research Online URL for this paper:

<https://eprints.whiterose.ac.uk/209854/>

Version: Published Version

Article:

Ali, H. orcid.org/0000-0001-6623-3374, Malik, M.Z., Abu-Farha, M. et al. (12 more authors) (2024) Global analysis of urinary extracellular vesicle small RNAs in autosomal dominant polycystic kidney disease. *The Journal of Gene Medicine*, 26 (2). e3674. ISSN 1099-498X

<https://doi.org/10.1002/jgm.3674>

Reuse

This article is distributed under the terms of the Creative Commons Attribution (CC BY) licence. This licence allows you to distribute, remix, tweak, and build upon the work, even commercially, as long as you credit the authors for the original work. More information and the full terms of the licence here:

<https://creativecommons.org/licenses/>

Takedown

If you consider content in White Rose Research Online to be in breach of UK law, please notify us by emailing eprints@whiterose.ac.uk including the URL of the record and the reason for the withdrawal request.




eprints@whiterose.ac.uk
<https://eprints.whiterose.ac.uk/>

RESEARCH ARTICLE

WILEY

Global analysis of urinary extracellular vesicle small RNAs in autosomal dominant polycystic kidney disease

Hamad Ali^{1,2,3}  | Md. Zubair Malik² | Mohamed Abu-Farha⁴ |
 Jehad Abubaker⁴ | Preethi Cherian⁴ | Rasheeba Nizam² | Sindhu Jacob² |
 Yousif Bahbahani^{3,5} | Medhat Naim³ | Sajjad Ahmad⁶ | Mohammad Al-Sayegh⁷ |
 Thangavel Alphonse Thanaraj² | Albert C. M. Ong⁸ | Peter C. Harris⁹ |
 Fahd Al-Mulla¹⁰

¹Department of Medical Laboratory Sciences, Faculty of Allied Health Sciences, Health Sciences Center (HSC), Kuwait University, Jabriya, Kuwait

²Department of Genetics and Bioinformatics, Dasman Diabetes Institute (DDI), Dasman, Kuwait

³Division of Nephrology, Mubarak Al-Kabeer Hospital, Ministry of Health, Jabriya, Kuwait

⁴Department of Biochemistry and Molecular Biology, Dasman Diabetes Institute (DDI), Dasman, Kuwait

⁵Medical Division, Dasman Diabetes Institute (DDI), Dasman, Kuwait

⁶UCL Institute of Ophthalmology, University College London, London, UK

⁷Biology Division, New York University Abu Dhabi, Abu Dhabi, United Arab Emirates

⁸Academic Nephrology Unit, Division of Clinical Medicine, School of Medicine and Population Health, Faculty of Health, University of Sheffield, Sheffield, UK

⁹Division of Nephrology and Hypertension, Mayo Clinic, Rochester, MN, USA

¹⁰Department of Translational Medicine, Dasman Diabetes Institute (DDI), Dasman, Kuwait

Correspondence

Hamad Ali, Department of Medical Laboratory Sciences, Faculty of Allied Health Sciences, Health Sciences Center (HSC), Kuwait University, Jabriya, Kuwait.
 Email: hamad.ali@ku.edu.kw

Funding information

Kuwait Foundation for the Advancement of Sciences (KFAS) grants, Grant/Award Numbers: PR17-13MM-07, RAHM-2019-030

Abstract

Background: Autosomal dominant polycystic kidney disease (ADPKD) is the most prevalent monogenic renal disease progressing to end-stage renal disease. There is a pressing need for the identification of early ADPKD biomarkers to enable timely intervention and the development of effective therapeutic approaches. Here, we profiled human urinary extracellular vesicles small RNAs by small RNA sequencing in patients with ADPKD and compared their differential expression considering healthy control individuals to identify dysregulated small RNAs and analyze downstream interaction to gain insight about molecular pathophysiology.

Methods: This is a cross-sectional study where urine samples were collected from a total of 23 PKD1-ADPKD patients and 28 healthy individuals. Urinary extracellular vesicles were purified, and small RNA was isolated and sequenced. Differentially expressed Small RNA were identified and functional enrichment analysis of the critical miRNAs was performed to identify driver genes and affected pathways.

Results: miR-320b, miR-320c, miR-146a-5p, miR-199b-3p, miR-671-5p, miR-1246, miR-8485, miR-3656, has_piR_020497, has_piR_020496 and has_piR_016271 were significantly upregulated in ADPKD patient urine extracellular vesicles and miRNA-29c was significantly downregulated. Five ‘driver’ target genes (*FBSR*, *EDC3*, *FMNL3*, *CTNNBIP1* and *KMT2A*) were identified.

Conclusions: The findings of the present study make significant contributions to the understanding of ADPKD pathogenesis and to the identification of novel biomarkers and potential drug targets aimed at slowing disease progression in ADPKD.

KEYWORDS

exosome, extracellular vesicles, miRNA, pi-RNA, polycystic kidney disease

This is an open access article under the terms of the [Creative Commons Attribution](https://creativecommons.org/licenses/by/4.0/) License, which permits use, distribution and reproduction in any medium, provided the original work is properly cited.

© 2024 The Authors. *The Journal of Gene Medicine* published by John Wiley & Sons Ltd.

1 | INTRODUCTION

Autosomal dominant polycystic kidney disease (ADPKD) is a renal monogenic disorder that affects approximately 1 in 1000 individuals and ranks as one of the leading causes of end stage renal disease in adults.^{1–3} ADPKD is characterized by a bilateral accumulation of fluid-filled cysts in the kidneys, leading to progressive enlargement of renal volume and a gradual decline in kidney function, often resulting in end stage renal disease.⁴ Besides the kidney-related symptoms, individuals with ADPKD might experience extrarenal manifestations including polycystic liver disease (PLD), cerebral aneurysms, and cardiovascular abnormalities, including early-onset hypertension.⁵ The majority of ADPKD cases (78%) are attributed to mutations in *PKD1*, whereas around 15% of the cases are caused by mutations in *PKD2* gene.⁶ Recently, *IFT140* has been suggested as the third most common gene linked to ADPKD cases,⁷ whereas other rarer forms of the disease have been linked to mutations in genes, including *GANAB*, *DNAJB11* and *ALG9*.^{8–10} This genetic heterogeneity has contributed to a wide phenotypic spectrum representing a challenge for disease diagnosis and prognosis, management of patients, genetic counseling, and patients' selection for clinical trials.^{11–13}

The most preferred method for monitoring ADPKD progression is the measurement of total kidney volume.¹⁴ However, this method is labor-intensive, which hinders its routine use in follow-ups. Mutation classification has been suggested as a means to identify patients at risk of the severe form of the disease; however, reports indicate that this cannot be done with complete certainty because of the modifying effects of other genetic and environmental factors.¹⁵ Currently, there are no reliable blood or urine biomarkers available that can accurately predict the course of the disease and identify patients at risk of the severe form of the disease. The presence of these biomarkers would enable improved management of patients and provide valuable support for clinical trials and the development of therapies.

Over the past decade, there has been a growing interest in exosomes, small extracellular vesicles with a diameter ranging between 40 and 160 nm derived from endosomes.¹⁶ These small vesicles contain various constituents including different types of nucleic acids (including microRNAs [miRNAs] and Piwi-interacting RNAs [piRNAs]), proteins, lipids, amino acids and other metabolites. Initially, extracellular vesicles were considered as cellular waste products resulting from cell damage or cell homeostasis¹⁷ but recent advances indicated that extracellular vesicles play a key role in intercellular communication that regulate major cellular processes including signal transduction and immune response.^{18,19} Extracellular vesicles are involved in cell–cell communication within the nephron influencing renal physiology and pathophysiology as their role have been implicated in various renal diseases and disorders including ADPKD.^{11,20,21} Studies have demonstrated the presence of altered extracellular vesicles profiles, in term of their nucleic acid and protein content, in various renal diseases including ADPKD.^{11,21} The extracellular vesicles content, specifically small non-coding RNAs, are considered to play a role in the pathogenesis of ADPKD by influencing various signaling

pathways through the post-transcriptional control of related genes.²² The pathologically modified extracellular vesicles profiles may provide potential biomarkers for disease diagnosis, prognosis and monitoring. They can also provide valuable insights for the development of potential therapies.

In the present study, we have taken a systematic approach to comprehensively profile the small RNA content of urinary extracellular vesicles from ADPKD patients and compared them with those from healthy individuals. We have identified significantly dysregulated miRNAs and piRNAs in ADPKD patients and compared the results to an independent global miRNA database of normal renal cortical tissue and PKD1 renal cysts. Additionally, we have further analyzed the network of common target mRNAs of the significantly dysregulated miRNAs. Our findings highlight potential novel biomarkers for ADPKD, identify potential therapeutic targets for the disease, and contribute to a better understanding of its pathophysiology.

2 | MATERIALS AND METHODS

2.1 | Patient recruitment

In total, 23 ADPKD patients were included in the present study. These patients were recruited from the nephrology unit at Mubarak Al-Kabeer Hospital and Mubarak Al-Abdullah Al-Sabah Dialysis Center in Jabriya. Eligible participants were adults over 18 years of age who were capable of providing informed consent. Inclusion criteria involved having a confirmed clinical diagnosis of ADPKD with positive genetic test. All patients had *PKD1* mutations that were reported previously.^{6,23,24} In addition, 28 healthy individuals were included in the study without any record of chronic health condition. The study received ethical approval from both the Ministry of Health (MOH) research ethics committee (Reference: 1139/2019) and the Joint Committee for The Protection of Human Subjects in Research of the Health Sciences Center (HSC) at Kuwait University and the Kuwait Institute for Medical Specialization (KIMS) (Reference: VDR/JC/690). Prior to participation, written informed consent was obtained from all enrolled patients in accordance with the guidelines set forth by the MOH research committee.

2.2 | Sample collection and exosome purification

Urine collection involved obtaining the first urine sample (50 ml) in urine collection and preservation tubes (50 ml) (18111) from Norgen Biotech Corp. (Thorold, ON, Canada). The collected tubes were subjected to a series of centrifugation steps. First, the tubes were centrifuged at 200 *g* for 20 min at 40°C to separate the supernatant. The supernatant was then transferred to a new 50-ml Falcon tube and centrifuged at 2000 *g* for 20 min at 40°C. Subsequently, the resulting supernatant was collected, and another centrifugation step was performed at 16,000 *g* for 20 min at 40°C. The supernatant

obtained was stored at 40°C. The remaining pellet was treated with 500 µl of dithiothreitol and subjected to vortexing and incubation at 37°C for 10 min. After incubation, the sample was centrifuged at 16,000 g for 20 min at 40°C. The supernatant from this step was combined with the stored supernatant from the previous step and filtered using a 0.2-µm filter. Equilibration of Amicon-15K filters was achieved by passing 15 ml of phosphate-buffered saline (PBS) and centrifuging at 3000 g for 25 min at 40°C. The filtered urine supernatant was loaded into the Amicon filter tubes and centrifuged at 3000 g for 45 min at 40°C, discarding the flow-through and repeating the process until the entire volume passed through the filter. This concentrated the sample and reduced its volume. The concentrated urine (approximately 500 µl) was transferred to ultracentrifuge tubes and centrifuged at 120 000 g for 70 min at 40°C. The supernatant was discarded, and the pellet was resuspended in 2 ml of PBS and centrifuged again at 120,000 g for 70 min at 40°C. Finally, the pellet was resuspended in 500 µl of PBS and stored overnight at 40°C.

2.3 | Total RNA extraction from urinary extracellular vesicles, library preparation and sequencing

RNA was extracted from urinary extracellular vesicles using a Urine Exosome Purification and RNA Isolation Maxi Kit (catalog. no, 58800; Norgen Biotech Corp.) in accordance with the manufacturer's instructions.

2.4 | Small RNA library preparation and sequencing

A total of 10 ng of purified small RNA samples was used for library preparation using a QIAseq miRNA Library Kit (331502; Qiagen, Hilden, Germany) in accordance with the manufacturer's instructions. The protocol involves sequential ligation of 3' and 5' end adapters followed by universal cDNA synthesis with unique molecular index assignment. Synthesized cDNA libraries were further amplified by PCR cycles and purified using Qiagen QMN beads. Prepared final libraries were validated and quantified using bioanalyzer (Agilent, Santa Clara, CA, USA) and qubit fluorometer (Thermo Fisher Scientific, Waltham, MA, USA) respectively. Sequencing was carried out on MiSeq system using Miseq 150 cycle version 3 kit (MS-102-3001; Illumina Inc. San Diego, CA, USA). The resulting Fastq files were analyzed using Gene globe data analysis webtools (Qiagen). Normalization was carried out using the trimmed mean of M (edgeR) method. A linear scaling factor for each sample was calculated from a weighted mean after reducing the dataset by log fold-changes relative to the control samples and by absolute intensity.²⁵ Candidate miRNAs were shortlisted using the criteria of log₂ fold change > 2 and $p < 0.05$.

2.5 | Annotation of small RNAs from sequencing data

FastQC software (Illumina, San Diego, California) was used to check the quality of Fastq files. Reads shorter than 14 nucleotides were discarded. Cutadapt v3.7 (<https://cutadapt.readthedocs.io/en/v3.7/guide.html>) was used to clip the reads that passed the quality control from the adapter sequences by imposing a maximum error rate in terms of mismatches, insertions and deletions equal to 0.15. The average length of the raw sRNA-seq reads was 22 bp. Trimmed reads were mapped against an in-house reference of human miRNA sequences composed of 1917 precursor miRNAs from miRBase v2274 (<https://mirbase.org/>). Using these settings, the seeding was not performed for reads shorter than 32 bp, and the reads were entirely evaluated for the alignment. miRNAs were annotated and quantified using two methods called the “knowledge-based” and “position-based” methods. In the “knowledge-based” method, the arm starting positions of the miRNA precursors were well defined. Based on the position of the mapped reads, it was possible to quantify the mature miRNAs. Alternatively, the “position-based” method was implemented for those miRNA precursors in which the positions of the 5p and 3p arms are not defined in miRBase. With the second method, based on the position of the read, it was assigned a “-5p” or “-3p” suffix to the name of miRNAs written in *italics* (to distinguish from the other miRNAs with assigned arms derived from miRBase). The quantification of mature miRNA annotations was performed by counting the read alignment reported by BWA output and an overall of 3524 miRNAs were analyzed. The results generated by the annotation and quantification methods were merged into a unique mature miRNA count matrix, composed of 3524 rows (miRNAs) and 335 columns (samples).

2.6 | Identification of differentially expressed small RNA (DE-sRNAs) and functional enrichment analysis of the critical miRNA

The validated miRNA-target mRNAs were retrieved using miRNet (www.mirnet.ca), an interactive web tool. The tool fetches miRNA-target interaction data (that are computationally predicted and experimentally validated) from miRTarBase,²⁶ miRDB²⁷ and TargetScan²⁸ databases. We considered the study miRNAs that are seen in these databases as candidate miRNAs in intersection with the mRNAs.²⁹ Significantly correlated pairs of such miRNA-mRNA interactions were utilized to generate the coexpression network using Cytoscape 3.6.1 (<https://cytoscape.org>). Significant biological pathways of significant candidate miRNAs were identified using the DIANA-microT web server.³⁰ The most statistically enriched Gene Ontology (GO) (<http://geneontology.org>) terms were visualized using the ggplot2 visualization package.³¹ The heatmap was plotted using SRPLOT (<https://www.bioinformatics.com.cn>).

2.7 | Comparison of miRNA expression in extracellular vesicles and PKD1 cystic tissues

miRNA expression data (GSE133530) from renal cysts of ADPKD patients is available in the database of Gene Expression Omnibus (GEO) (<https://www.ncbi.nlm.nih.gov/geo>) under accession number of GSE133530. The GSE133530 dataset comprises miRNA expression data from normal renal cortical tissue ($n = 4$), minimally cystic tissue ($n = 7$) and ADPKD renal cyst ($n = 18$) kidney samples. We retrieved the dataset and compared miRNA expression in exosome tissue from our ADPKD patients with miRNA expression in renal cyst tissues from the GSE133530 dataset. We obtained DE-miRNA from GSE133530 dataset using the GEO2R tool provided by the GEO database (<https://www.ncbi.nlm.nih.gov/geo/geo2r>). Only miRNAs implicated in cystic tissues and our ADPKD samples were considered for subsequent analysis to identify driver target genes.

2.8 | Identification of driver target genes of key miRNA

The cytoHubba v.0.1 plug-in of Cytoscape was used to select potential hub genes from the identified DE-miRNAs.^{32,33} The bottleneck centrality analysis of the miRNA-mRNA regulatory network was used to determine the driver genes that are targeted by the key miRNA.^{34,35}

2.9 | Statistical analysis

We calculated receiver operating characteristic (ROC) curves. These curves compare sensitivity versus specificity across a range of values for the ability to predict a dichotomous outcome. Area under the ROC curve (AUC) is another measure of test performance. We calculated the AUC, confidence intervals, p values of all calculated ROC curves and the ROC curves for each individual piRNA and miRNA, and displayed them along their corresponding sensitivity and specificity.

3 | RESULTS

3.1 | Expression profiles of miRNAs isolated from urinary extracellular vesicles of ADPKD patients

Characterization of purified urinary extracellular vesicles based on size using different microscopic modalities showed a diameter in the range of 40–150 nm (see Supporting information, Figure S1A–C). Flow cytometry analysis indicated that extracellular vesicles exhibited positive expression of CD63 and TSC-101 and negative expression of GRP94 (see Supporting information, Figure S1D).

Urinary extracellular vesicles small RNAs were extracted from individuals ($n = 51$). The cohort included 28 healthy controls with normal kidney function and 23 ADPKD patients with known PKD1 mutations. The baseline and clinical characteristics of the ADPKD patients and controls are shown in Table 1. The expression profiles of urinary extracellular vesicles small RNAs from the 23 ADPKD patients were compared with the expression profiles from the 28 healthy individuals. Principal component analysis of the small RNA expression data demonstrated clustering of ADPKD patients and healthy controls with a separation between the two clusters (Figure 1A). Results of heatmap clustering based on the expression pattern of all 318 detectable miRNAs and piRNAs of healthy and ADPKD groups are presented in the Supporting information (Table S1). Transcript cluster heatmaps (Figure 1B) indicated that the optimal number of clusters was eight; the larger cluster ($n = 52$ miRNAs and piRNA) was designated C2 and the smaller cluster ($n = 23$ miRNAs and piRNA) was designated C1 (see Supporting information, Table S1). Clusters C3, C6 and C8 revealed the same changes in the expression of miRNA/piRNAs in healthy and ADPKD. Clusters C1 and C4 revealed higher expression of miRNA/piRNAs in ADPKD patients, whereas clusters C2, C5 and C7 revealed lower expression of miRNA/piRNAs in ADPKD patients (see Supporting information, Table S1).

Differential expression analysis revealed that 32 (out of 318) miRNAs ($n = 9$) and piRNAs ($n = 23$) were significantly differentially expressed between healthy controls and ADPKD patients with $p < 0.05$ (Figure 1C). We found nine miRNAs to be significantly dysregulated between control individuals and ADPKD patients; eight miRNAs (i.e. miR-8485, miR-671-5p, miR-3656, miR-320c, miR-320b, miR-199b-3p, miR-146a-5p and miR-1246) were overexpressed in ADPKD patients and one (i.e. miR-29c-3p) was downregulated in ADPKD patients. We also observed that 23 extracellular vesicles piRNAs were differentially expressed; 20 piRNAs were overexpressed

TABLE 1 Basic demographic and clinical characteristics of the study cohort.

Characteristic	Healthy controls ($n = 28$)	ADPKD patients ($n = 23$)
Sex (M:F)	15:13	13:10
Age, mean (SD) (years)	62 (6.3)	39 (12.02)
BMI, mean (SD) (kg/m^2)	33 (6)	27.2 (4.16)
eGFR, mean (SD) ($\text{ml}/\text{min}/1.73\text{m}^2$)	ND	75.71 (37.08)
Total Kidney Volume (TKV), mean (SD) (ml)	ND	1360.01 (800.47)
Serum creatinine, mean (SD) ($\mu\text{mol}/\text{L}$)	82 (20)	127.73(130.04)

Abbreviations: ADPKD, autosomal dominant polycystic kidney disease; BMI, body mass index; eGFR, estimated glomerular filtration rate; F, female; M, male; ND, undetermined.

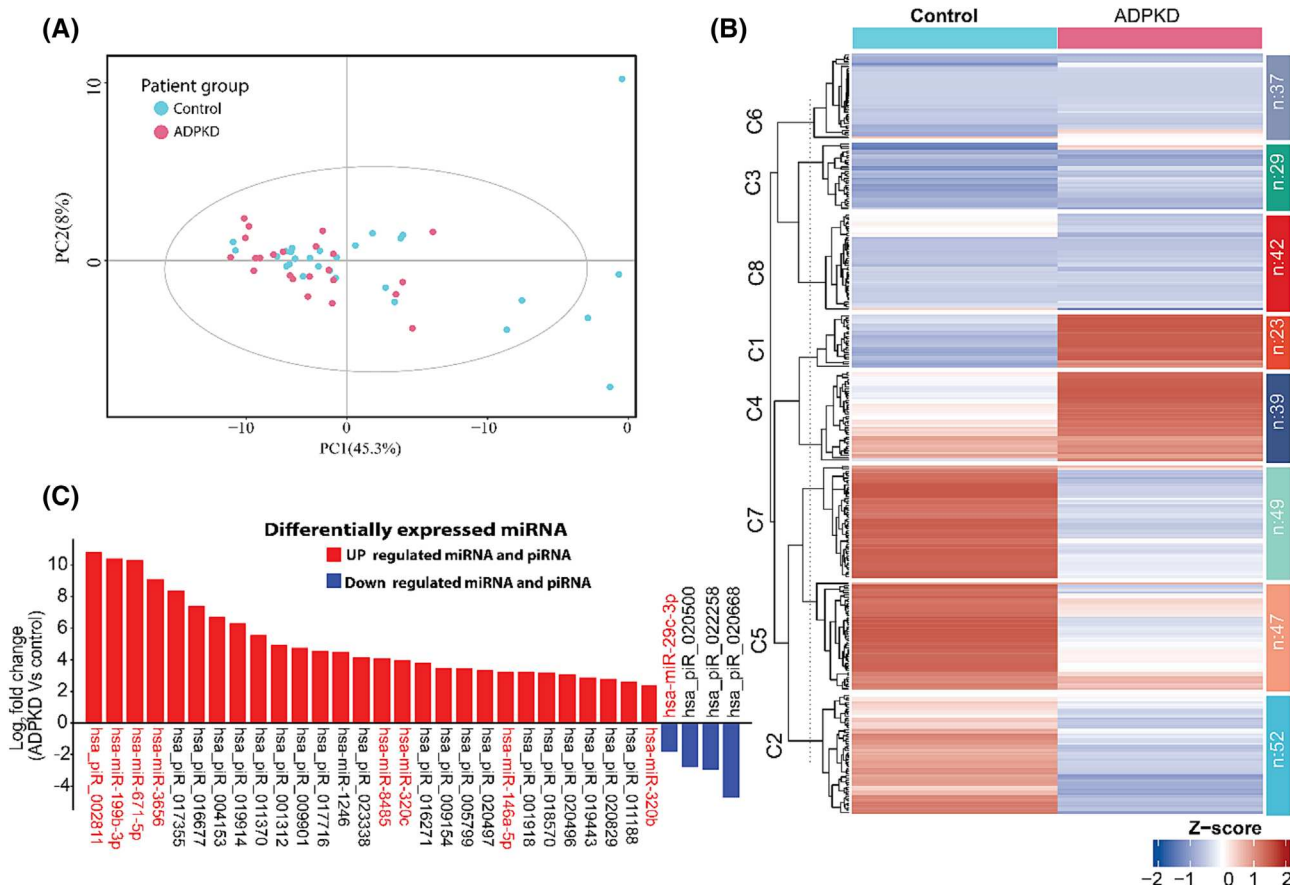


FIGURE 1 Expression profile of urinary extracellular vesicles small RNAs. (A) Principal component analysis of the miRNA expression data from healthy controls and autosomal dominant polycystic kidney disease (ADPKD). (B) Heatmap of the differentially expressed urinary extracellular vesicles small miRNAs in healthy control and ADPKD patient. (C) Expression of differentially expressed urinary extracellular vesicles small miRNAs and piRNAs in individual healthy control and ADPKD patients. The red text denotes the miRNA and the black text is piRNA.

in ADPKD patients and three were downregulated in ADPKD patients, as shown in Figure 1C.

3.2 | Dysregulated small RNAs in ADPKD urinary extracellular vesicles

The heatmap clustering of DE-sRNA expression is presented in Figure 2A. Clustering indicated that the difference in miRNA and piRNA expression levels between control individuals and ADPKD patients is the primary discriminator, overriding differences as a result of gender, age and body mass index (BMI). The nine extracellular vesicles miRNAs, which were shown to be differentially expressed between control and ADPKD individuals, were further analyzed using Wilcoxon rank sum tests. The results of Wilcoxon tests pointed to a relationship between BMI and miRNA expression in patients with ADPKD (see Supporting information, Figure S2A). For example, the expressions of miR-199b, miR-320c and miR-1246 were significantly and negatively correlated with BMI with a correlation coefficient of -0.34 ($p = 0.014$), -0.29 ($p = 0.04$) and -0.33 ($p = 0.018$), respectively (see Supporting information,

Figure S2B). Additionally, the expressions of miR-320c, miR-199b and miR-1246 were significantly correlated with age (correlation coefficient of -0.28 ($p = 0.048$), -0.28 ($p = 0.045$) and -0.32 ($p = 0.021$)), respectively (see Supporting information, Figure S3). As regards the expression of miR-29c, a strong positive correlation was seen between its expression and age of the ADPKD patients with a correlation coefficient of 0.41 ($p = 0.003$) (see Supporting information, Figure S3).

A significant change in expression was seen with miR-29c-3p ($p = 0.00043$), miR-320c (0.0051), miR-1246 ($p = 0.0093$), miR-671-5p ($p = 0.024$) and miR-8485 ($p = 0.04$) in ADPKD patients compared to control individuals (Figure 2B). No significant difference was observed in the abundance of miR-146a-5p ($p = 0.53$), miR-199b-3p ($p = 0.21$), miR-3656 ($p = 0.12$) and miR-320b ($p = 0.11$) between ADPKD patients and control individuals (Figure 2B). A significant change in expression was seen with piR_020497 ($p = 0.002$), piR_016271 ($p = 0.01$) and piR_020496 ($p = 0.03$) in ADPKD patients compared to control individuals (see Supporting information, Figure S4A).

Next, by considering the estimated glomerular filtration rate (eGFR), we divided the ADPKD cohort ($n = 23$) into two groups: one

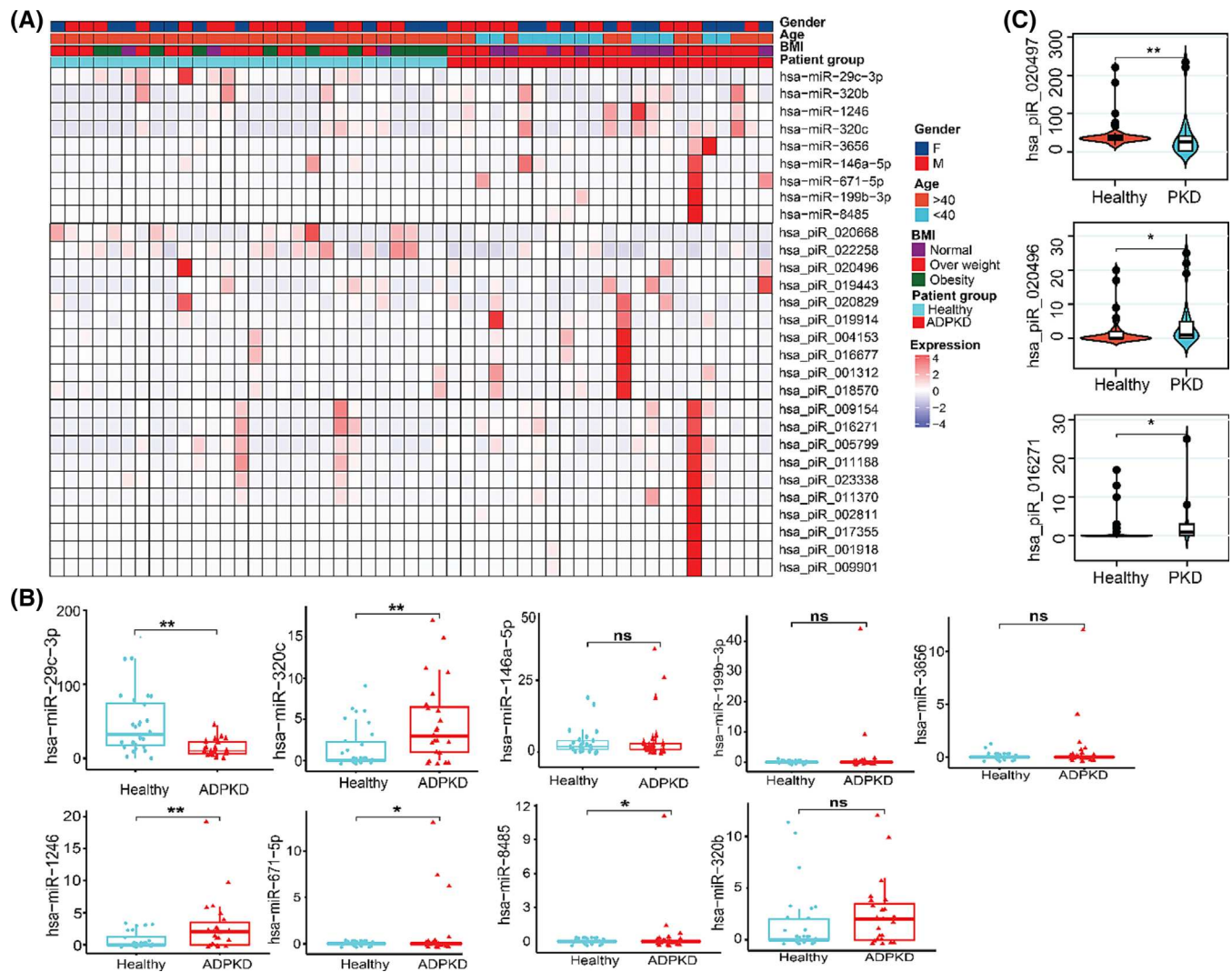


FIGURE 2 (A) Heatmap of DE-miRNAs between transcriptomes and clinical phenotypic, either between gender, age and BMI. Expression values for each miRNA (row) are normalized across ADPKD and control samples (columns) by Z-score. Expression levels of miRNAs are shown in red (upregulated) and blue (downregulated), with brighter shades indicating higher fold differences (\log_{10} fold change values). The lack of difference in expression levels is represented in white. (B) Expression of individual miRNAs by normalized (norm) signal values between healthy controls and ADPKD patients. * $p < 0.05$ and ** $p < 0.01$. ns, not significant. (C) Expression of individual significant urinary exosome piRNAs by norm signal values between healthy controls and ADPKD patients. * $p < 0.05$ and ** $p < 0.01$.

with $\text{eGFR} > 60 \text{ ml/min per } 1.73 \text{ m}^2$, indicating milder or early renal impairment ($n = 14$), and the second group with $\text{eGFR} \leq 60 \text{ ml/min per } 1.73 \text{ m}^2$, denoting severe/late renal disease ($n = 9$), and compared them with the healthy control group ($n = 28$). Heatmaps displayed separation of these three groups, with the lowest expression of multiple miRNAs evident with the ADPKD group of severe/late renal disease (i.e. with $\text{eGFR} \leq 60 \text{ ml/min per } 1.73 \text{ m}^2$) (Figure 3A). ADPKD patients with early disease (i.e. with $\text{eGFR} > 60 \text{ ml/min per } 1.73 \text{ m}^2$) had significantly higher expression of miR-29c-3p ($p = 0.0029$), miR-199b ($p = 0.043$), miR-671-5p ($p = 0.024$) and miR-8485 ($p = 0.048$) compared to healthy control individuals (Figure 3B). Additionally, ADPKD patients with late disease ($\text{eGFR} \leq 60 \text{ ml/min per } 1.73 \text{ m}^2$) had significantly higher expression of miR-320b ($p = 0.0092$), miR-320c ($p = 0.0063$) and miR-1246 ($p = 0.014$) compared to

healthy control individuals (Figure 3B) and significantly lower expression of miR-29c-3p ($p = 0.0088$) compared to healthy control individuals (Figure 3B).

3.3 | The potential diagnostic value of urinary extracellular vesicles miRNAs for ADPKD

Results of ROC curve analysis evaluating the potential diagnostic value of the urinary extracellular vesicles miRNAs, which showed significantly different expression between the ADPKD patients and healthy individuals, are presented in Figure 3C. Levels of miR-29-3p, miR-320b, miR-320c, and miR-1246 could clearly distinguish the ADPKD patients from healthy individuals. Compared to

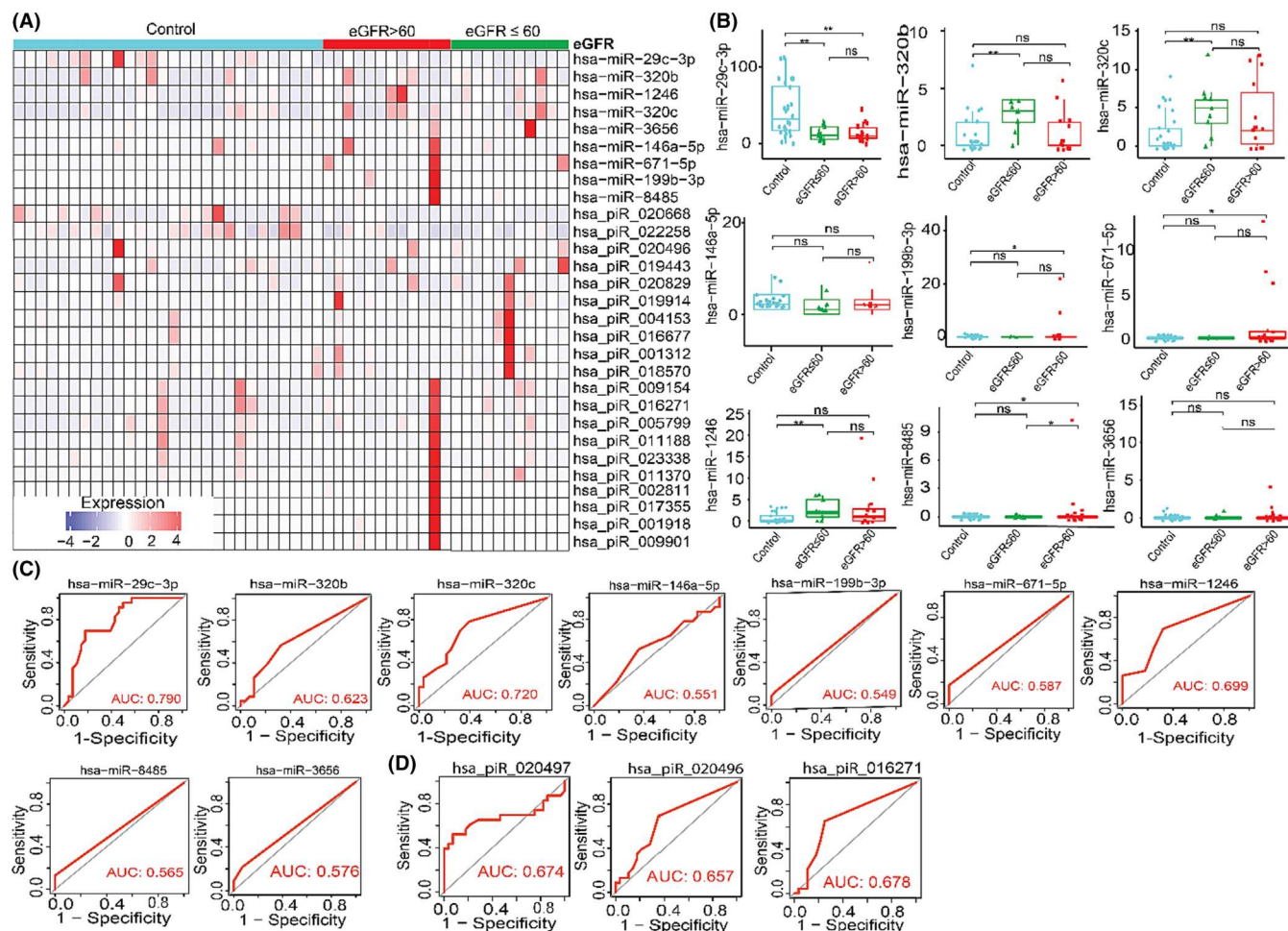


FIGURE 3 (A) Heatmap showing expression profiles of differentially expressed urinary extracellular vesicles miRNAs in healthy control and ADPKD patients with early (eGFR > 60 ml/min per 1.73 m²) and late (eGFR ≤ 60 ml/min per 1.73 m²). (B) Expression of individual urinary extracellular vesicles miRNAs by normal signal values between healthy controls and ADPKD patients with early (eGFR > 60 ml/min per 1.73 m²) and late (eGFR ≤ 60 ml/min per 1.73 m²) renal disease. **p* < 0.05 and ***p* < 0.01. ns, not significant. (C) ROC curve for miRNA-29c, miR-320b, miR-320c, miR-146a-5p, miR-199b-3p, miR-671-5p, miR-1246, miR-8485 and miR-3656 based on the miRNA expression data. (D) ROC curve for significant piRNA (has_piR_020497, has_piR_020496 and has_piR_016271) based on the piRNA expression data. The diagram plots the sensitivity (true-positive rate) versus specificity (false-positive rate). The AUC values indicate that the patient groups with differing eGFR in ADPKD and controls may be distinguished by the expression analysis of the markers.

controls, miR-29c-3p with an AUC value of 0.790 (close to be qualified as “excellent”) had the largest area under the ROC curve with the highest sensitivity and specificity compared to the other three considered miRNAs; namely, miR-320c (AUC = 0.720), miR-320b (AUC = 0.623) and miR-1246 (AUC = 0.699) (Figure 3C). The miR-320c also has an “acceptable” AUC value of 0.720. Furthermore, compared to controls, piR_020497, piR_016271 and piR_020496 in ADPKD with AUC values of 0.674, 0.678 and 0.657, respectively, had areas under the ROC curve with the sensitivities and specificities observed (see Supporting information, Figure S4B). The AUC values indicate that individuals with differing eGFR in ADPKD and control groups can be distinguished by the expression analysis of the markers. These data indicate that these miRNAs are valuable potential urinary-based miRNA biomarkers not only for ADPKD, but also for detecting future renal impairment in ADPKD patients.

3.4 | Validation of urinary exosome miRNA expression via comparison to PKD1 renal cystic tissues

To validate our cohort findings, we analyzed the data available in the GEO database on miRNA expression from PKD1 renal cystic tissues obtained from ADPKD patients. Thirty-one differentially expressed miRNAs that we found shared between our urinary extracellular vesicles miRNAs and miRNAs from PKD1 cystic tissues (Figure 4A). Heat maps further displayed expression pattern of these 31 miRNAs in normal, minimally cystic tissue (MCT) and PKD1 renal cystic tissue groups (Figure 4B). We found that seven dysregulated urinary extracellular vesicles miRNAs (viz. miR-29c-3p, miR-671-5p, miR-320c, miR-320b, miR-199b-3p, miR-146a-5p and miR-1246) are also significantly expressed in cystic tissues of PKD1 (Figure 4C). miR-199b-3p is significantly overexpressed in MCT and PKD1 renal cystic tissue, but, in urinary exosome, the expressed was non-significant. We also

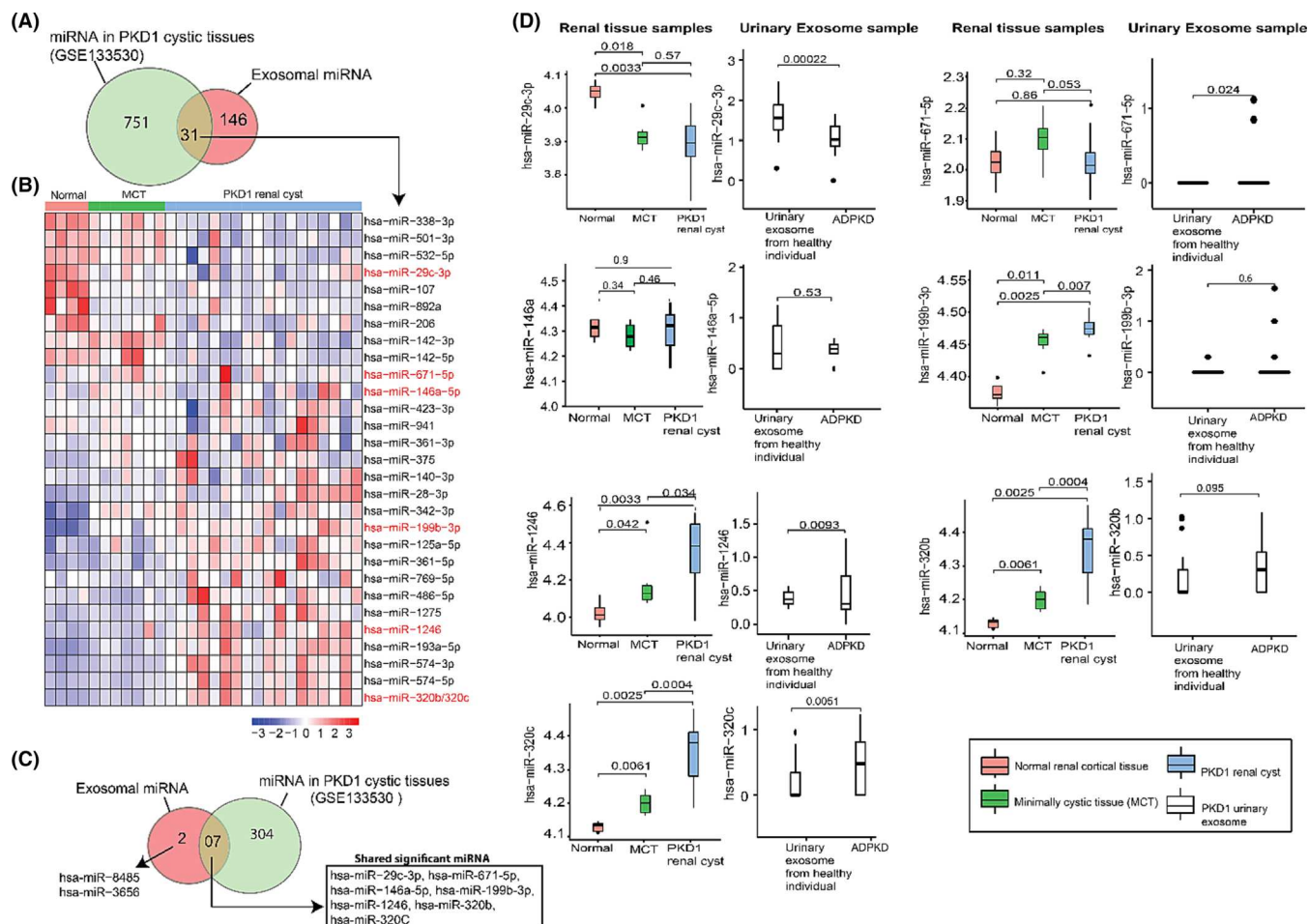


FIGURE 4 Validation of differentially expressed urinary extracellular vesicles microRNAs (miRNAs) in urine samples from human renal cyst tissue sample. (A) Venn diagram showing shared miRNAs between urinary extracellular vesicles miRNA and PKD1 cystic tissues from dataset GSE133530 from gene expression omnibus (GEO). (B) Heatmap showing expression profiles of DE-miRNAs in human renal cyst tissue among three groups: normal renal cortical ($n = 4$), minimally cystic ($n = 18$) and PKD1 renal cyst ($n = 7$) samples. The red color character shows the significant differentially urinary extracellular vesicles miRNA. (C) Venn diagram shows shared significant differentially expressed miRNAs between urinary extracellular vesicles miRNA and PKD1 cystic tissues from dataset GSE133530 from GEO. (D) Differential expressions of miR-29c, miR-199b-3p, miR-320b, miR-320c, miR-146a, miR-1246 and miR-671-5p in human PKD1 tissue samples and exosome.

observed that miR-8485 and miR-3656 are significant unique urinary exosomal miRNA (Figure 4C). Significant increases in the expression levels of miR-1246, miR-320b and miR-320c were found in MCT, PKD1 renal cystic tissue and urinary exosome compared to normal tissue (Figure 4D). Additionally, a significant decrease in the expression levels of miR-29c-3p was observed in MCT, PKD1 renal cystic tissue and urinary exosome compared to normal tissue. We also observed, in two of the miRNAs (i.e. miR-146a-5p and miR-671) that showed no dysregulation in ADPKD urinary extracellular vesicles, a similar pattern across the MCT cystic tissues and PKD1 renal cystic tissue compared to healthy cyst (Figure 4D).

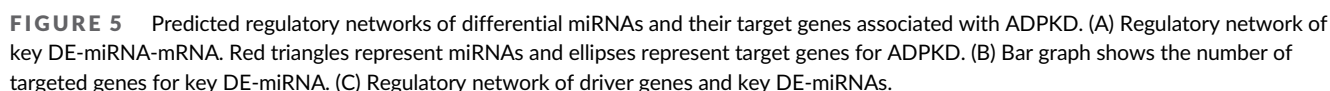
3.5 | Prediction of target genes of extracellular vesicles miRNAs

miRNAs play a significant role in modulating mRNA expression levels within cells. They achieve this by binding to target mRNAs and leading

to translational repression and gene silencing. The detected 318 differentially expressed miRNAs (including the identified nine dysregulated miRNAs in urinary extracellular vesicles from ADPKD patients) were found to map to 846 target genes in the miRNet database (see Supporting information, Table S2). The protein-protein interaction network built using the differentially expressed miRNA-mRNA pairs revealed that the interaction network comprises 846 interacting nodes and 949 edges. The regulatory network of four significant dysregulated miRNAs that is expressed in urinary extracellular vesicles as well as cystic tissues of PKD1 (i.e. miR-29c-3p, miR-671-5p, miR-320c and miR-1246) and predicted genes is given in Figure 5A.

3.6 | Identification of the driver gene from miRNA-mRNA regulatory network in ADPKD

Of the interacting miRNA-mRNA pairs, four DE-miRNAs (i.e. miR-29c-3p, miR-671-5p, miR-320c and miR-1246) mapped to kidney-



identified by DAVID (<https://david.ncicrf.gov/tools.jsp>) to validate that these miRNAs are involved in ADPKD. Enrichment analysis revealed that the targeted genes were enriched mainly in mitogen-activated protein kinase signaling (mTOR), Wnt signaling, phosphoinositide 3-kinase (PI3K)-Akt signaling, apoptosis, MAPK signaling, p53 signaling, calcium signaling and ErbB signaling pathways (Figure 6A; see also Supporting information, Table S3). Of interest, the top ADPKD-associated pathways of most of the extracellular vesicles key miRNAs families were related to Wnt signaling, mTOR, ErbB signaling, PI3K-Akt and calcium signaling (Figure 6B). In addition, more specific participation in APKD-related biological process analysis showed that the enriched processes were involved in cell proliferation, hypoxia, nephrogenesis, cell migration, cell differentiation, fibrosis and DNA damage (Figure 5C). Figure 6D shows the PI3K-Akt signaling pathway associated with target genes of extracellular vesicles miRNAs.

4 | DISCUSSION

In the present study, we employed a systematic approach to comprehensively profile small RNAs from ADPKD patients' urinary extracellular vesicles using the NGS platform. The dysregulated miRNAs and piRNA were analyzed to explore their potential as disease biomarkers.

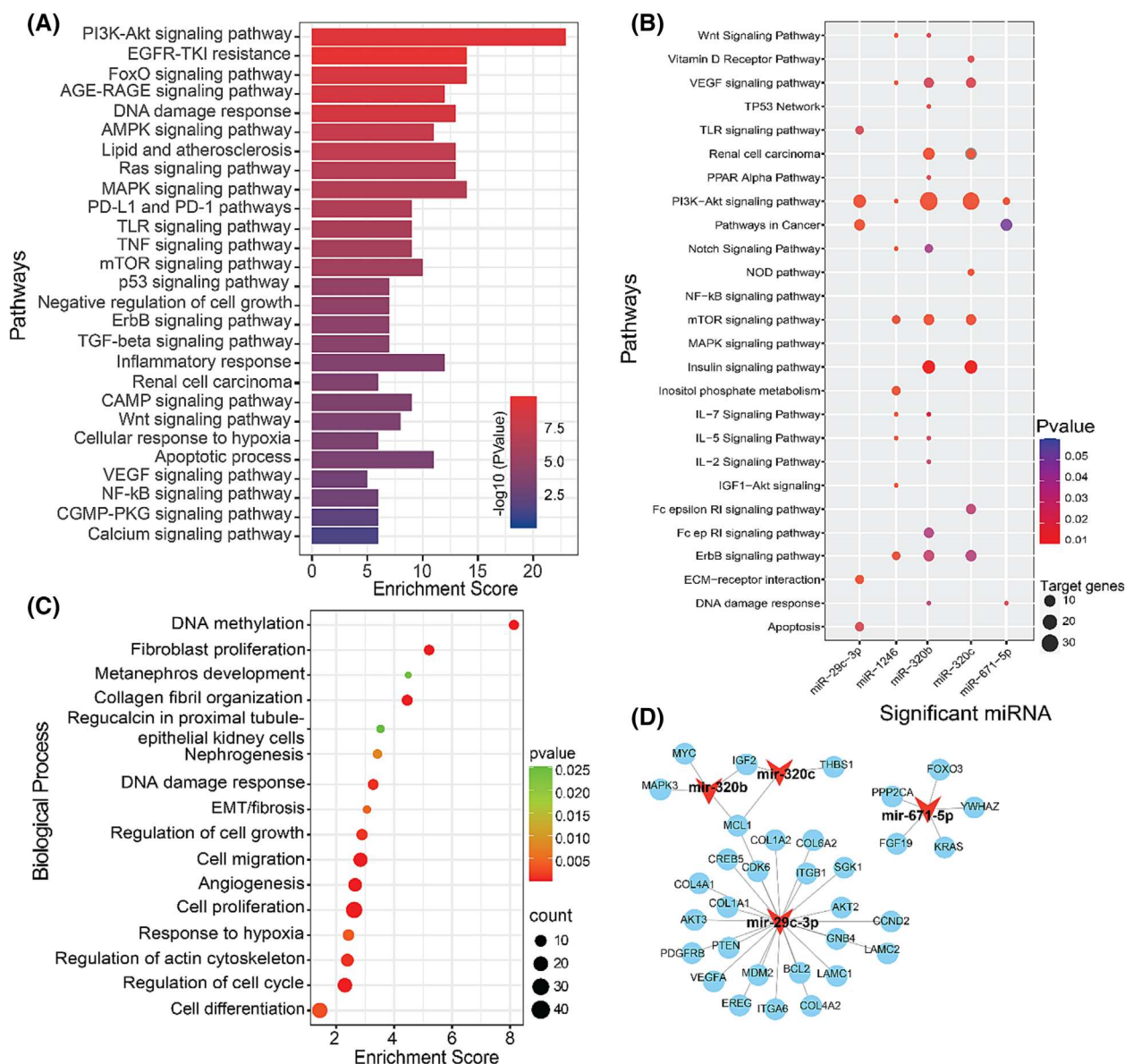


FIGURE 6 Functional enrichment analysis of DE-miRNA. (A) Bar plot of significant biological pathways of targeted genes to DE-miRNA. X-axes represent count with significance ($p < 0.05$) indicated by order and color trend. (B) The functional enrichment findings for the targets of the significant DE-miRNAs are shown as dot plots, with the y-axis revealing the annotation classifications, the x-axis presenting the miRNAs, and the number of identified targets in a circle also shown. The size of the dots corresponds to the gene ratio, whereas the colored dots indicate adjusted p -values. (C) Significantly enriched biological process of targeted genes. Dot size indicates the count. The count represents the number of genes associated with each process. The dot color denotes the p -values of the process, and the x-axis represents the fold enrichment score. (D) PI3K-Akt signaling pathways associated with target genes of extracellular vesicles miRNAs.

Furthermore, we validated our findings by comparing them with miRNA expression data (GSE133530) from renal cysts of ADPKD patients that were retrieved from the NCBI GEO database. To identify interaction networks and driver target genes of the key dysregulated miRNAs, we utilized both computationally predicted and experimentally validated databases. These analyses provided valuable insights into ADPKD pathophysiology and potential therapeutic directions. Overall, our research sheds light on the regulatory role of miRNAs in ADPKD and highlights their relevance as potential biomarkers and targets for potential therapeutic interventions.

piRNAs comprise small non-coding silencing RNAs with a length range from 21 to 35 nucleotides and have been shown to have distinct protein-interaction dynamics when compared to miRNAs.³⁶ They are known to be involved in regulation of genomic stability in animal cells³⁷ and their profiles have been shown to be dysregulated renal cell carcinomas.³⁸ To our knowledge, this is the first study evaluating piRNAs profiles and their diagnostic potential in ADPKD. We have identified 23 dysregulated piRNAs in ADPKD patients with only three of them showing statistical significance (i.e. piR_020497, piR_016271 and piR_020496). The AUC-ROC curves for these piRNAs showed

similar outcomes with limited potential in predicting the ADPKD cases. Further studies are required to fully evaluate their potential in clinical practice.

We have identified nine miRNAs (i.e. miR-8485, miR-671-5p, miR-3656, miR-320c, miR-320b, miR-199b-3p, miR-146a-5p, miR-1246 and miR-29c-3p) isolated from urinary extracellular vesicles that are significantly dysregulated between healthy controls and ADPKD. None of these identified DE-miRNAs were reported previously to be linked directly to ADPKD. However, a few of them have shown involvement in other renal pathological processes, whereas the remainder were implicated in certain types of cancer. Two of the detected DE-miRNAs were associated with diabetic nephropathy. miR-8485, isolated from circulating extracellular vesicles, was previously shown to be downregulated in diabetic nephropathy patients.³⁹ Meanwhile, miR-320c was found to be overexpressed in urinary extracellular vesicles of diabetic nephropathy patients.⁴⁰ miR-199b-3p has been shown to have a protective role in acute kidney injury because it inhibits oxidative stress,⁴¹ whereas miR-146a-5p has been shown to act as a mediator of renal tubular response to ischemia-reperfusion injury, thereby suppressing the accompanied inflammation.⁴² On the other hand, miR-671-5p, miR-3656 and miR-1246, which were significantly elevated in our ADPKD extracellular vesicles renal samples, were shown previously to play a role in renal and lung carcinomas.^{43–45} This is not surprising because the PI3K/Akt/mTOR pathway, which regulates cell growth and survival, is implicated in both ADPKD-related renal cyst growth and tumor growth in various types of cancer.⁴⁶ miR-29c-3p, in particular, showed an interesting pattern where it was significantly downregulated in ADPKD urinary extracellular vesicles compared to the healthy individuals. This particular miRNA have been shown to be downregulated in renal fibrosis,⁴⁷ which is one of the physiological contributors to ADPKD progression.⁴⁸ This particular marker was also shown to be downregulated in PKD1 cystic tissue (Figure 6C) and its potential diagnostic was implicated the ROC curve analysis (Figure 3). Furthermore, functional enrichment analysis indicated the miR-29c-3p to target a large set of 254 genes that participate in ADPKD-related pathways, including PI3K-Akt and mTOR⁴⁹ (Figure 5; see also Supporting information, Figure S5 and Table S3). Similar functional enrichment was noted for miRNAs (miR-199b-3p, miR-29c-3p, miR-320b, miR-320c and miR-146a-5p) (see Supporting information, Table S3). Magayr et al.²¹ previously explored the dysregulated miRNA in ADPKD urinary extracellular vesicles. Compared with their results, we found that three of our nine extracellular vesicles miRNAs were differentially expressed in a their study; specifically, hsa-miR-320b (eGFR late stage, \log_2 FC 1.02, $p = 0.037$) and hsa-miR-1246 (eGFR early stage, \log_2 FC 2.26, $p = 0.014$) were increased, whereas hsa-miR-199b-3p (eGFR late stage, \log_2 FC -3.75, $p = 0.007$) was decreased in ADPKD patients compared to healthy volunteers. A similar strong link to PI3K-Akt was also identified though it was linked to different set of miRNAs.²¹ The observed differences can be attributed to the heterogenous nature of ADPKD itself, disparities in laboratory methodologies and the nature of the specimen. The influence of a patient's ethnicity might have a limited impact, but it cannot be entirely ruled out.

Furthermore, by examining the miRNet database, we were able to identify potential mRNA targets from kidney tissue recognized by differentially expressed extracellular vesicles miRNAs and to identify pathways enriched by the target mRNAs. The constructed regulatory networks of miRNA-mRNA (target genes) revealed a total of four key DE-miRNAs targeting five driver genes; namely, *FMNL3*, *KMT2A*, *EDC3*, *FBR5* and *CTNNBIP1*; these five driver genes corresponded to the top nodes having highest degree and bottleneck in the constructed network. We found that miR-29c-3p, which showed significant downregulation in the ADPKD exosome, interacted with four of the five driver genes; namely, *FMNL3*, *EDC3*, *FBR5* and *CTNNBIP1*. The *FMNL3* driver gene is targeted by both miR-29c-3p and miR-671-5p, the *KMT2A* gene by miR-671-5p, and the *EDC3* gene is targeted by both miR-1246 and miR-320c.

EDC3 is involved in regulation of gene expression, and it has been shown that suppressing the phosphorylation of *EDC3* reduces tumor growth and invasion, and thereby drives cancer progression.⁵⁰ *KMT2A* is also involved in regulation of gene expression and is implicated in different types of leukemia.⁵¹ *FMNL3* plays a significant role in actin polymerization,^{52,53} regulating cell migration, metastasis and tumor progression.⁵⁴ *CTNNBIP1* encodes a negative regulator of the Wnt signaling pathway⁵⁵ and as the Wnt signaling pathway has been shown to be disrupted in cystic kidney, a potential connection could be hypothesized.

The study has the following limitations. A significant challenge lies in the computational prediction of miRNA-target genes because the miRNet, TargetScan and miRbase tools are prone to predicting notable proportion of false-positive interactions. This issue arises partly as a result of the context-dependent nature of posttranscriptional regulation. To address this, researchers have proposed integrating target predictions from multiple tools because increasing experimental evidence supports the hypothesis that miRNAs can act through target degradation. This approach may help identify miRNA/mRNA relationships more accurately. The findings of the present study were reached by applying an integrative system biology approach; hence, the results need to be interpreted with caution and future experimental studies are required to fully understand the molecular mechanisms underlying ADPKD.

5 | CONCLUSIONS

Our comprehensive approach revealed a number of differentially expressed urinary extracellular vesicles piRNA miRNAs and their target genes participating in the progression of ADPKD in humans. The present study provides an interpretation of the biological processes and pathways enriched by these markers. The study indicated that multiple miRNAs may regulate a single mRNA, and a single miRNA may target hundreds of different genes. Further integration of these data into gene regulatory networks may reveal the cooperative translational control mechanisms in cells. The study shortlisted nine 'key' differentially expressed miRNAs and five 'driver' target genes regulating the progression of ADPKD in humans, and these have the

potential to serve as biomarkers for disease progression and as therapeutic targets for ADPKD. Our findings significantly contribute to the understanding of ADPKD's pathogenesis and to the identification of novel biomarkers and potential drug targets aimed at slowing disease progression in ADPKD.

AUTHOR CONTRIBUTIONS

HA was responsible for study conception, study design, coordination of the study and funding acquisition. HA, MdZM, MA-S, TAT and FA-M were responsible for the interpretation of data. HA and MdZM were responsible for writing the manuscript. MdZM was responsible for data analysis. MA-F and JA were responsible for data acquisition. PC, RN and SJ were responsible for experimental work. YB and MN were responsible for patient diagnosis and recruitment. SA was responsible for the design of the sample purification methodology. TAT and FA-M were responsible for revising the manuscript. ACO was responsible for data validation. PCH was responsible for diagnostic data acquisition. All authors have approved the submitted version of the manuscript and agreed both to be personally accountable for the author's own contributions and to ensure that questions related to the accuracy or integrity of any part of the work are appropriately addressed.

ACKNOWLEDGMENTS

We extend our appreciation to the Kuwait Foundation for the Advancement of Science (KFAS) administration for their invaluable support in advancing medical research in Kuwait. This study was funded by KFAS grants (PR17-13MM-07) awarded to H.A. and (RA HM-2019-030) for the Kuwait Adult Diabetes Epidemiology Multidisciplinary (KADEM) program.

CONFLICT OF INTEREST STATEMENT

The authors declare that they have no conflicts of interest.

DATA AVAILABILITY STATEMENT

The data underlying this article will be available from the corresponding author upon reasonable request.

ETHICAL STATEMENT

The study received ethical approval from both the Ministry of Health (MOH) research ethics committee (Reference: 1139/2019) and the Joint Committee for The Protection of Human Subjects in Research of the Health Sciences Center (HSC) at Kuwait University and the Kuwait Institute for Medical Specialization (KIMS) (Reference: VDR/JC/690). Before participation, written informed consent was obtained from all enrolled patients per the guidelines set forth by the MOH research committee.

TRANSLATIONAL STATEMENT

Our analysis has revealed a significant dysregulation of both miRNAs and pi-RNAs in urinary extracellular vesicles of ADPKD patients, which such findings being are particularly compelling compared to an independent global miRNA database comprising normal renal cortical

tissue and PKD1 renal cysts. Furthermore, we have delved deeper into understanding the functional implications of these dysregulated small RNAs by elucidating the network of common target mRNAs associated with the significantly dysregulated miRNAs. These multifaceted findings collectively underscore the potential of our study to serve as a valuable resource for identifying novel biomarkers for ADPKD, elucidating potential therapeutic targets and enhancing our overall comprehension of the disease's pathophysiology.

ORCID

Hamad Ali  <https://orcid.org/0000-0001-6623-3374>

REFERENCES

1. Suwabe T, Shukoor S, Chamberlain AM, et al. Epidemiology of autosomal dominant polycystic kidney disease in Olmsted county. *Clin J Am Soc Nephrol*. 2020;15(1):69-79. doi:[10.2215/CJN.05900519](https://doi.org/10.2215/CJN.05900519)
2. Cornec-Le Gall E, Alam A, Perrone RD. Autosomal dominant polycystic kidney disease. *Lancet*. 2019;393(10174):919-935. doi:[10.1016/S0140-6736\(18\)32782-X](https://doi.org/10.1016/S0140-6736(18)32782-X)
3. Aung TT, Bhandari SK, Chen Q, et al. Autosomal dominant polycystic kidney disease prevalence among a racially diverse United States population, 2002 through 2018. *Kidney360*. 2021;2(12):2010-2015. doi:[10.34067/KID.0004522021](https://doi.org/10.34067/KID.0004522021)
4. Bergmann C, Guay-Woodford LM, Harris PC, Horie S, Peters DJM, Torres VE. Polycystic kidney disease. *Nat Rev Dis Primers*. 2018;4(1):50. doi:[10.1038/s41572-018-0047-y](https://doi.org/10.1038/s41572-018-0047-y)
5. Luciano RL, Dahl NK. Extra-renal manifestations of autosomal dominant polycystic kidney disease (ADPKD): considerations for routine screening and management. *Nephrol Dial Transplant*. 2014;29(2):247-254. doi:[10.1093/ndt/gft437](https://doi.org/10.1093/ndt/gft437)
6. Ali H, Naim M, Senum SR, et al. The genetic landscape of autosomal dominant polycystic kidney disease in Kuwait. *Clin Kidney J*. 2023;16(2):355-366. doi:[10.1093/ckj/sfac236](https://doi.org/10.1093/ckj/sfac236)
7. Senum SR, Li YSM, Benson KA, et al. Monoallelic IFT140 pathogenic variants are an important cause of the autosomal dominant polycystic kidney-spectrum phenotype. *Am J Hum Genet*. 2022;109(1):136-156. doi:[10.1016/j.ajhg.2021.11.016](https://doi.org/10.1016/j.ajhg.2021.11.016)
8. Besse W, Chang AR, Luo JZ, et al. ALG9 mutation carriers develop kidney and liver cysts. *J Am Soc Nephrol*. 2019;30(11):2091-2102. doi:[10.1681/ASN.2019030298](https://doi.org/10.1681/ASN.2019030298)
9. Porath B, Gainullin VG, Cornec-Le Gall E, et al. Mutations in GANAB, encoding the glucosidase Ila subunit, cause autosomal-dominant polycystic kidney and liver disease. *Am J Hum Genet*. 2016;98(6):1193-1207. doi:[10.1016/j.ajhg.2016.05.004](https://doi.org/10.1016/j.ajhg.2016.05.004)
10. Huynh VT, Audrezet MP, Sayer JA, et al. Clinical spectrum, prognosis and estimated prevalence of DNAJB11-kidney disease. *Kidney Int*. 2020;98(2):476-487. doi:[10.1016/j.kint.2020.02.022](https://doi.org/10.1016/j.kint.2020.02.022)
11. Hogan MC, Bakeberg JL, Gainullin VG, et al. Identification of biomarkers for PKD1 using urinary exosomes. *J Am Soc Nephrol*. 2015;26(7):1661-1670. doi:[10.1681/ASN.2014040354](https://doi.org/10.1681/ASN.2014040354)
12. Bais T, Gansevoort RT, Meijer E. Drugs in clinical development to treat autosomal dominant polycystic kidney disease. *Drugs*. 2022;82(10):1095-1115. doi:[10.1007/s40265-022-01745-9](https://doi.org/10.1007/s40265-022-01745-9)
13. Ali H, Alahmad B, Senum SR, et al. PKD1 truncating mutations accelerate eGFR decline in autosomal dominant polycystic kidney disease patients. *Am J Nephrol*. 2024;1-9. doi:[10.1159/000536165](https://doi.org/10.1159/000536165)
14. Perrone RD, Mouksassi MS, Romero K, et al. Total kidney volume is a prognostic biomarker of renal function decline and progression to end-stage renal disease in patients with autosomal dominant polycystic kidney disease. *Kidney Int Rep*. 2017;2(3):442-450. doi:[10.1016/j.ekir.2017.01.003](https://doi.org/10.1016/j.ekir.2017.01.003)

15. Lanktree MB, Guiard E, Li W, et al. Intrafamilial variability of ADPKD. *Kidney Int Rep.* 2019;4(7):995-1003. doi:[10.1016/j.ekir.2019.04.018](https://doi.org/10.1016/j.ekir.2019.04.018)
16. Kalluri R, LeBleu VS. The biology, function, and biomedical applications of exosomes. *Science.* 2020;367(6478):1-15. doi:[10.1126/science.aau6977](https://doi.org/10.1126/science.aau6977)
17. Thery C, Zitvogel L, Amigorena S. Exosomes: composition, biogenesis and function. *Nat Rev Immunol.* 2002;2(8):569-579. doi:[10.1038/nri855](https://doi.org/10.1038/nri855)
18. Mittelbrunn M, Gutierrez-Vazquez C, Villarroya-Beltri C, et al. Unidirectional transfer of microRNA-loaded exosomes from T cells to antigen-presenting cells. *Nat Commun.* 2011;2(1):282. doi:[10.1038/ncomms1285](https://doi.org/10.1038/ncomms1285)
19. Gangoda L, Boukouris S, Liem M, Kalra H, Mathivanan S. Extracellular vesicles including exosomes are mediators of signal transduction: are they protective or pathogenic? *Proteomics.* 2015;15(2-3):260-271. doi:[10.1002/pmic.201400234](https://doi.org/10.1002/pmic.201400234)
20. Stahl PD, Raposo G. Extracellular vesicles: exosomes and microvesicles. *Integrators of Homeostasis Physiology (Bethesda).* 2019;34(3):169-177. doi:[10.1152/physiol.00045.2018](https://doi.org/10.1152/physiol.00045.2018)
21. Magayr TA, Song X, Streets AJ, et al. Global microRNA profiling in human urinary exosomes reveals novel disease biomarkers and cellular pathways for autosomal dominant polycystic kidney disease. *Kidney Int.* 2020;98(2):420-435. doi:[10.1016/j.kint.2020.02.008](https://doi.org/10.1016/j.kint.2020.02.008)
22. Zheng Q, Reid G, Eccles MR, Stayner C. Non-coding RNAs as potential biomarkers and therapeutic targets in polycystic kidney disease. *Front Physiol.* 2022;13:1006427. doi:[10.3389/fphys.2022.1006427](https://doi.org/10.3389/fphys.2022.1006427)
23. Ali H, Hussain N, Naim M, et al. A novel PKD1 variant demonstrates a disease-modifying role in trans with a truncating PKD1 mutation in patients with autosomal dominant polycystic kidney disease. *BMC Nephrol.* 2015;16(1):26. doi:[10.1186/s12882-015-0015-7](https://doi.org/10.1186/s12882-015-0015-7)
24. Ali H, Al-Mulla F, Hussain N, et al. PKD1 duplicated regions limit clinical utility of whole exome sequencing for genetic diagnosis of autosomal dominant polycystic kidney disease. *Sci Rep.* 2019;9(1):4141. doi:[10.1038/s41598-019-40761-w](https://doi.org/10.1038/s41598-019-40761-w)
25. Robinson MD, McCarthy DJ, Smyth GK. edgeR: a Bioconductor package for differential expression analysis of digital gene expression data. *Bioinformatics.* 2010;26(1):139-140. doi:[10.1093/bioinformatics/btp616](https://doi.org/10.1093/bioinformatics/btp616)
26. Hsu JT, Peng CH, Hsieh WP, Lan CY, Tang CY. A novel method to identify cooperative functional modules: study of module coordination in the *Saccharomyces cerevisiae* cell cycle. *BMC Bioinformatics.* 2011;12(1):281. doi:[10.1186/1471-2105-12-281](https://doi.org/10.1186/1471-2105-12-281)
27. Wang X. miRDB: a microRNA target prediction and functional annotation database with a wiki interface. *RNA.* 2008;14(6):1012-1017. doi:[10.1261/ma.965408](https://doi.org/10.1261/ma.965408)
28. Lewis BP, Burge CB, Bartel DP. Conserved seed pairing, often flanked by adenosines, indicates that thousands of human genes are microRNA targets. *Cell.* 2005;120(1):15-20. doi:[10.1016/j.cell.2004.12.035](https://doi.org/10.1016/j.cell.2004.12.035)
29. Khan MM, Serajuddin M, Malik MZ. Identification of microRNA and gene interactions through bioinformatic integrative analysis for revealing candidate signatures in prostate cancer. *Gene Reports.* 2022;27:101607. doi:[10.1016/j.genrep.2022.101607](https://doi.org/10.1016/j.genrep.2022.101607)
30. Shannon P, Markiel A, Ozier O, et al. Cytoscape: a software environment for integrated models of biomolecular interaction networks. *Genome Res.* 2003;13(11):2498-2504. doi:[10.1101/gr.1239303](https://doi.org/10.1101/gr.1239303)
31. Wickham H. ggplot2. *WIREs Computational Statistics.* 2011;3(2):180-185. doi:[10.1002/wics.147](https://doi.org/10.1002/wics.147)
32. Lalwani AK, Krishnan K, Bagabir SA, et al. Network theoretical approach to explore factors affecting signal propagation and stability in dementia's protein-protein interaction network. *Biomolecules.* 2022;12(3):451. doi:[10.3390/biom12030451](https://doi.org/10.3390/biom12030451)
33. Chin C-H, Chen S-H, Wu H-H, Ho C-W, Ko M-T, Lin C-Y. cytoHubba: identifying hub objects and sub-networks from complex interactome. *BMC Syst Biol.* 2014;8(4):S11. doi:[10.1186/1752-0509-8-S4-S11](https://doi.org/10.1186/1752-0509-8-S4-S11)
34. Iqbal S, Malik MZ, Pal D. Network-based identification of miRNAs and transcription factors and in silico drug screening targeting δ -secretase involved in Alzheimer's disease. *Heliyon.* 2021;7(12):e08502. doi:[10.1016/j.heliyon.2021.e08502](https://doi.org/10.1016/j.heliyon.2021.e08502)
35. Banaganapalli B, Al-Rayes N, Awan ZA, et al. Multilevel systems biology analysis of lung transcriptomics data identifies key miRNAs and potential miRNA target genes for SARS-CoV-2 infection. *Comput Biol Med.* 2021;135:104570. doi:[10.1016/j.combiomed.2021.104570](https://doi.org/10.1016/j.combiomed.2021.104570)
36. Ozata DM, Gainetdinov I, Zoch A, O'Carroll D, Zamore PD. PIWI-interacting RNAs: small RNAs with big functions. *Nat Rev Genet.* 2019;20(2):89-108. doi:[10.1038/s41576-018-0073-3](https://doi.org/10.1038/s41576-018-0073-3)
37. Siomi MC, Sato K, Pezic D, Aravin AA. PIWI-interacting small RNAs: the vanguard of genome defence. *Nat Rev Mol Cell Biol.* 2011;12(4):246-258. doi:[10.1038/nrm3089](https://doi.org/10.1038/nrm3089)
38. Ding L, Wang R, Xu W, et al. PIWI-interacting RNA 57125 restrains clear cell renal cell carcinoma metastasis by downregulating CCL3 expression. *Cell Death Discov.* 2021;7(1):333. doi:[10.1038/s41420-021-00725-4](https://doi.org/10.1038/s41420-021-00725-4)
39. Kim H, Bae YU, Jeon JS, et al. The circulating exosomal microRNAs related to albuminuria in patients with diabetic nephropathy. *J Transl Med.* 2019;17(1):236. doi:[10.1186/s12967-019-1983-3](https://doi.org/10.1186/s12967-019-1983-3)
40. Delic D, Eisele C, Schmid R, et al. Urinary exosomal miRNA signature in type II diabetic nephropathy patients. *PLoS ONE.* 2016;11(3):e0150154. doi:[10.1371/journal.pone.0150154](https://doi.org/10.1371/journal.pone.0150154)
41. Tian X, Liu Y, Wang H, et al. The role of miR-199b-3p in regulating Nrf2 pathway by dihydromyricetin to alleviate septic acute kidney injury. *Free Radic Res.* 2021;55(7):842-852. doi:[10.1080/10715762.2021.1962008](https://doi.org/10.1080/10715762.2021.1962008)
42. Amrouche L, Desbuissons G, Rabant M, et al. MicroRNA-146a in human and experimental ischemic AKI: CXCL8-dependent mechanism of action. *J Am Soc Nephrol.* 2017;28(2):479-493. doi:[10.1681/ASN.2016010045](https://doi.org/10.1681/ASN.2016010045)
43. Chi XG, Meng XX, Ding DL, et al. HMGA1-mediated miR-671-5p targets APC to promote metastasis of clear cell renal cell carcinoma through Wnt signaling. *Neoplasia.* 2020;67(1):46-53. doi:[10.4149/neo_2019_190217N135](https://doi.org/10.4149/neo_2019_190217N135)
44. Zaravinos A, Lambrou GI, Mourmouras N, et al. New miRNA profiles accurately distinguish renal cell carcinomas and upper tract urothelial carcinomas from the normal kidney. *PLoS ONE.* 2014;9(3):e91646. doi:[10.1371/journal.pone.0091646](https://doi.org/10.1371/journal.pone.0091646)
45. Zhang WC, Chin TM, Yang H, et al. Tumour-initiating cell-specific miR-1246 and miR-1290 expression converge to promote non-small cell lung cancer progression. *Nat Commun.* 2016;7(1):11702. doi:[10.1038/ncomms11702](https://doi.org/10.1038/ncomms11702)
46. Seeger-Nukpezah T, Geynisman DM, Nikonova AS, Benzing T, Golemis EA. The hallmarks of cancer: relevance to the pathogenesis of polycystic kidney disease. *Nat Rev Nephrol.* 2015;11(9):515-534. doi:[10.1038/nrneph.2015.46](https://doi.org/10.1038/nrneph.2015.46)
47. Macak N, Jovanovic I, Zivkovic M, et al. Downregulation of fibrosis related hsa-miR-29c-3p in human CAKUT. *Nucleosides Nucleotides Nucleic Acids.* 2023;42(12):945-958. doi:[10.1080/15257770.2023.2218430](https://doi.org/10.1080/15257770.2023.2218430)
48. Norman J. Fibrosis and progression of autosomal dominant polycystic kidney disease (ADPKD). *Biochim Biophys Acta.* 2011;1812(10):1327-1336. doi:[10.1016/j.bbdis.2011.06.012](https://doi.org/10.1016/j.bbdis.2011.06.012)
49. Harris PC, Torres VE. Genetic mechanisms and signaling pathways in autosomal dominant polycystic kidney disease. *J Clin Invest.* 2014;124(6):2315-2324. doi:[10.1172/JCI72272](https://doi.org/10.1172/JCI72272)
50. Bearss JJ, Padi SK, Singh N, et al. EDC3 phosphorylation regulates growth and invasion through controlling P-body formation and dynamics. *EMBO Rep.* 2021;22(4):e50835. doi:[10.15252/embr.202050835](https://doi.org/10.15252/embr.202050835)
51. Meyer C, Larghero P, Almeida Lopes B, et al. The KMT2A recombinome of acute leukemias in 2023. *Leukemia.* 2023;37(5):988-1005. doi:[10.1038/s41375-023-01877-1](https://doi.org/10.1038/s41375-023-01877-1)

52. Phng LK, Gebala V, Bentley K, et al. Formin-mediated actin polymerization at endothelial junctions is required for vessel lumen formation and stabilization. *Dev Cell*. 2015;32(1):123-132. doi:[10.1016/j.devcel.2014.11.017](https://doi.org/10.1016/j.devcel.2014.11.017)
53. Thompson ME, Heimsath EG, Gauvin TJ, Higgs HN, Kull FJ. FMNL3 FH2-actin structure gives insight into formin-mediated actin nucleation and elongation. *Nat Struct Mol Biol*. 2013;20(1):111-118. doi:[10.1038/nsmb.2462](https://doi.org/10.1038/nsmb.2462)
54. Bai SW, Herrera-Abreu MT, Rohn JL, et al. Identification and characterization of a set of conserved and new regulators of cytoskeletal organization, cell morphology and migration. *BMC Biol*. 2011;9(1):54. doi:[10.1186/1741-7007-9-54](https://doi.org/10.1186/1741-7007-9-54)
55. Liu J, Xiao Q, Xiao J, et al. Wnt/beta-catenin signalling: function, biological mechanisms, and therapeutic opportunities. *Signal Transduct Target Ther*. 2022;7(1):3. doi:[10.1038/s41392-021-00762-6](https://doi.org/10.1038/s41392-021-00762-6)

SUPPORTING INFORMATION

Additional supporting information can be found online in the Supporting Information section at the end of this article.

How to cite this article: Ali H, Malik MZ, Abu-Farha M, et al. Global analysis of urinary extracellular vesicle small RNAs in autosomal dominant polycystic kidney disease. *J Gene Med*. 2024;26(2):e3674. doi:[10.1002/jgm.3674](https://doi.org/10.1002/jgm.3674)